Catalysis Today 151 (2010) 285–290

Contents lists available at ScienceDirect

Catalysis Today

journal homepage: www.elsevier.com/locate/cattod

Pd-promoted catalysts for low temperature diesel engine DeNO$_x$

B. Greenhalgh, J.-P. Charland, M. Stanciulescu*, R. Burich, J. Kelly

CanmetENERGY – Innovation and Energy Technology Sector, Natural Resources Canada, 1 Haanel Drive, Ottawa, Ontario K1A 1M1, Canada

ARTICLE INFO

Article history:
Available online 20 April 2010

Keywords:
DeNO$_x$
Syngas
SCR
Sol–gel
Aftertreatment

ABSTRACT

A series of promoted Pd catalysts supported on a mixed γ-Al_2O_3–TiO_2 support was prepared for use in selective catalytic reduction (SCR) of nitrogen oxides (NO$_x$) using hydrogen rich syngas as a reductant. The catalysts, containing Pd, Fe, Co and K incorporated through incipient wetness, were characterized in terms of surface area, elemental composition and crystalline chemical phase. The NO$_x$ reduction (DeNO$_x$) activity of the catalyst series was measured as a function of temperature in a flow reactor system fed with a simulated diesel engine exhaust. The catalyst series shows high NO$_x$ conversion and favorable selectivity to N_2 over a wide range of temperature compared to results on similar catalyst systems reported to date.

1. Introduction

NO and NO_2 (collectively termed NO$_x$) are the primary oxides of nitrogen. They are produced in significant quantities during combustion processes and are known to have serious impacts on the environment. These effects include the formation of acid rain, particulate matter and photochemical smog, as well as stratospheric ozone depletion and ground level ozone formation [1]. Correspondingly, environmental legislation places severe restrictions on the allowable NO$_x$ content in diesel engine exhaust. For example, the 2010 EPA Tier 2 Bin 5 emission standards for light duty diesel engines demand NO$_x$ levels below 0.05 g/mi [2].

To address these challenges, internal combustion engine manufacturers have made significant progress in suppressing the formation of NO$_x$. Such advancements, including Exhaust Gas Recycling (EGR) and Homogeneous Charge Compression Ignition (HCCI), are well described elsewhere in the literature [3,4]. Nonetheless, meeting the increasingly stringent environmental legislation will require the addition of aftertreatment technologies for the reduction of NO$_x$ to N_2 (DeNO$_x$). One such option is the catalytic reduction of NO$_x$, which can be broadly divided into NO$_x$ storage and reduction (NSR), and selective catalytic reduction (SCR). NSR systems typically consist of a NO$_x$ adsorbing phase such as BaO and a NO$_x$ reduction phase such as Pt, while SCR technology aims to reduce NO$_x$ species as they exit the engine [1]. Such catalysts consist of metals supported on either high surface area materials, such as zeolites and γ-Al_2O_3, or on thermo-mechanically stable honeycomb materials as cordierite. Another feature of SCR systems is that a reductant is required.

While such after-treatment technologies show promise in meeting the increasingly stringent limits on NO$_x$ emissions, each has its own limitations. For example, NO$_x$ traps are highly susceptible to poisoning by sulfur species in fuels and lubricating oil [1]. In the case of SCR systems, sufficient NO$_x$ reduction activity is difficult to achieve in lean combustion applications [5–10].

Ammonia is widely used as a reductant in lean NO$_x$ control technology, particularly in stationary applications [5,7,9,10]. However, the use of NH_3 (or derivatives thereof) as reductants is made impractical by several issues. These include such as NH_3 slip [5,10], the formation of byproducts such as ammonium nitrate [11] as well as the need to store and inject NH_3 into the exhaust stream [5,9,10]. Many researchers are thus focusing on the development of onboard reductant generation [5,7–10]. The most obvious area of focus would be on hydrocarbons. Pt has been reported to be a most promising catalyst for this application [5,8,10]. The use of hydrocarbon reductants is limited however by insufficient NO$_x$ reduction activity at low temperature and by poor N_2 selectivity, leading to N_2O formation [7,8,10]. Hydrogen, which is also present within the exhaust stream of lean combustion processes, shows promise as a superior reductant to hydrocarbons in the presence of Pt catalysts. It offers higher activity at low temperature than hydrocarbons, but also exhibits low N_2 selectivity, leading to high N_2O production [5–10]. Furthermore, unless H_2 could be generated on-board, the same arguments against using NH_3 in mobile applications could be applied to H_2. For this reason, there is a considerable interest in developing SCR technology based on the use of syngas (a mixture of H_2 and CO which is produced through incomplete combustion) as a reductant [9]. While such an approach provides a means of supplying H_2, Pt catalysts are poisoned by the strong adsorption of CO [5–10]. In contrast, Pd is not poisoned by CO. In fact, CO behaves as a NO$_x$ reductant over Pd catalysts, and higher activity is reported for syngas mixtures compared to either pure H_2 or CO [5]. Motivated by previous literature reports on the varied activity of Pt supported on

---

* Corresponding author. Tel.: +1 613 943 0103; fax: +1 613 996 9400.
E-mail address: mstanciu@nrcan.gc.ca (M. Stanciulescu).

0920-5861/$ – see front matter. Crown Copyright © 2010 Published by Elsevier B.V. All rights reserved.
doi:10.1016/j.cattod.2010.03.035

Table 1
Nominal metal loadings on γ-Al_2O_3–TiO_2.

Catalyst name	Nominal loading (mass %)			
	Pd	Fe	Co	K
Pd/Al_2O_3–TiO_2	0.5	0.0	0.0	0.0
Pd/K/Al_2O_3–TiO_2	0.5	0.0	0.0	0.5
Pd/Co/Al_2O_3–TiO_2	0.5	0.0	0.5	0.0
Pd/K/Co/Al_2O_3–TiO_2	0.5	0.0	0.5	0.5
Pd/Fe/Al_2O_3–TiO_2	0.5	1.5	0.0	0.0

SiO_2 and Al_2O_3 [12] mixed oxides [13] as well as Pd on TiO_2, Al_2O_3, SiO_2 and MgO [14] using pure hydrogen as a reductant, Macleod and Lambert [6] reported on the improved activity of Pd supported on 10% TiO_2 dispersed on Al_2O_3. Konsolakis et al. [10] extended this work by investigating the use of potassium as a promoter of Pd on such supports in an effort to improve activity over a wider range of temperatures. These authors report high NO_x conversion and N_2 selectivity.

Finally, an interesting discussion can be found in the literature on the formation of *in situ* reductants and intermediates. For example, Ueda et al. [14] discuss the formation and subsequent reduction of NO_2 while Macleod and Lambert [7,8] and Macleod et al. [9] discuss the formation of formate, isocyanates and possibly NH_3 on Pd/Al_2O_3 in the presence of H_2, NO and O_2. Konsolakis et al. [10] confirm the formation of NH_3 on the surface of potassium promoted Pd on Al_2O_3/TiO_2.

In the present study, we report novel extensions to the existing literature in this area. First, we consider the use of doubly promoted Pd catalysts, using K, Co and Fe in an attempt to improve low temperature activity and maximize N_2 selectivity. In addition, the testing of all our catalysts was conducted in the presence of 5% H_2O, which is more realistic of engine exhaust conditions.

2. Experimental

2.1. Catalyst preparation

A mixed γ-Al_2O_3–TiO_2 support was prepared by dispersing titania (TiO_2) on high surface area γ-Al_2O_3. The high surface area γ-Al_2O_3 was prepared by the modified sol–gel method described by Maunula et al. [15]. Specifically, 120 g of 2-methylpentane-2,4-diol was mixed with 108 g of aluminum isopropoxide and stirred for 4 h at 120 °C. After lowering the temperature to 100 °C and adding 90 g of water, the mixture was stirred vigorously for 2 h, after which it was then allowed to stand overnight at 80 °C. The resulting slurry was dried under vacuum using a rotary evaporator and then placed in an oven overnight at 120 °C. The resulting γ-Al_2O_3 product was calcined at 500 °C for 6 h in air. TiO_2 was deposited as a monolayer on the high surface area γ-Al_2O_3 (270 m^2/g) in a ratio of Al_2O_3/TiO_2 equal to 4. This resulted in a mixed support of 80% Al_2O_3–20% TiO_2. Further details of the deposition procedure can be found in the work of Macleod and Lambert [6]. A higher amount of TiO_2 was deposited on alumina in our preparation to account for the fact that Lambert used γ-Al_2O_3 of lower surface area (100 m^2/g) [6]. The resulting support, Al_2O_3–TiO_2, was loaded with Pd, Fe, Co and K (as aqueous nitrates) through the method of incipient wetness. The catalysts were prepared with metal loadings ranging from 0.5% to 1.5% (by mass), and, in the case of promoted catalysts, they were named in such a way as to indicate the order of metal incorporation. For example, Pd/K/Co/Al_2O_3–TiO_2 was prepared by first incorporating Co, then K and finally Pd, with a drying step of 120 °C for 16 h and a calcination step of 500 °C for 6 h, both in air, following the incorporation of *each* metal. The description and nominal loadings of the catalysts prepared in this study are listed in Table 1.

2.2. Catalyst characterization

Sample compositions were determined using a Hitachi S3400N VP-SEM operating at 20 kV and 80 mA under vacuum and coupled to an Oxford INCA EDS detector system. Preparation consisted of a thin layer of powdered sample held in place with double-sided carbon tape. For each sample, 10 points from different regions were measured to produce an average and a standard deviation of the composition.

The BET surface areas of the catalysts were measured using a Micromeritics ASAP 2020 instrument by nitrogen adsorption at −196 °C. Each sample was degassed for 16 h at 200 °C before the isotherms were measured.

The crystalline chemical phase compositions of the prepared catalysts and the Al_2O_3–TiO_2 support were verified by X-ray diffraction (XRD). XRD patterns of the samples were collected on a Siemens D500TT diffractometer, employing a CuK_α source ($\lambda = 1.54$ Å), and equipped with a diffracted-beam graphite monochromator and a scintillation detector. The XRD data were processed using JADE Plus version 7.5 software. The detected phases were identified using the search/match option in JADE database. The XRD spectra were also visually matched using XRD patterns in the powder diffraction file PDF-2 from the International Centre for Diffraction Data (ICDD).

2.3. Catalytic activity

Each sample was ground to a fine powder and then pressed into thin (ca. 1 mm) wafers under 7 tons of pressure. After lightly crushing these wafers in a mortar and pestle, the particles were sieved within a size range of 80–120 mesh. The particles were then loaded into a flow reaction system as depicted in Fig. 1. The relevant operating parameters are as follows:

- Catalyst mass: ca. 500 mg
- Gas hourly space velocity (GHSV): 95,000 h^{-1}
- Negative temperature ramp: 450–300 °C at 2 °C/min; 300–75 °C at 1 °C/min
- Feed: 500 ppm NO, 5% O_2, 5% H_2O, 0.3% H_2, 0.1% CO in He

The analytical instrumentation on the catalyst testing unit includes online measurement of gaseous reaction products using a Innova 1301 photoacoustic FTIR spectrometer. It is driven by ROM software loaded in an integrated computer. This software can perform IR spectrum measurement, spectral calibration and quantitative monitoring of target gases through pre-selected spectral windows. Other specific details of the reaction system can be found in previously published literature [16].

3. Results and discussion

3.1. Characterization

3.1.1. SEM/EDS

The nominal and measured loadings of the active metals on the support are shown in Tables 1 and 2. With regard to the standard deviation, the measured compositions are in reasonably good agreement with the nominal loadings (Table 1) employed during preparation, with the exception of the Pd/Fe catalyst. It is possible that such a high loading of metals on this particular catalyst resulted in surface agglomeration, which may have resulted in higher composition by SEM. The standard deviations corresponding to the support metals compositions are high (0.6) compared to those of the promoter elements (0.02–0.1), but on a percentage basis these deviations are comparable.

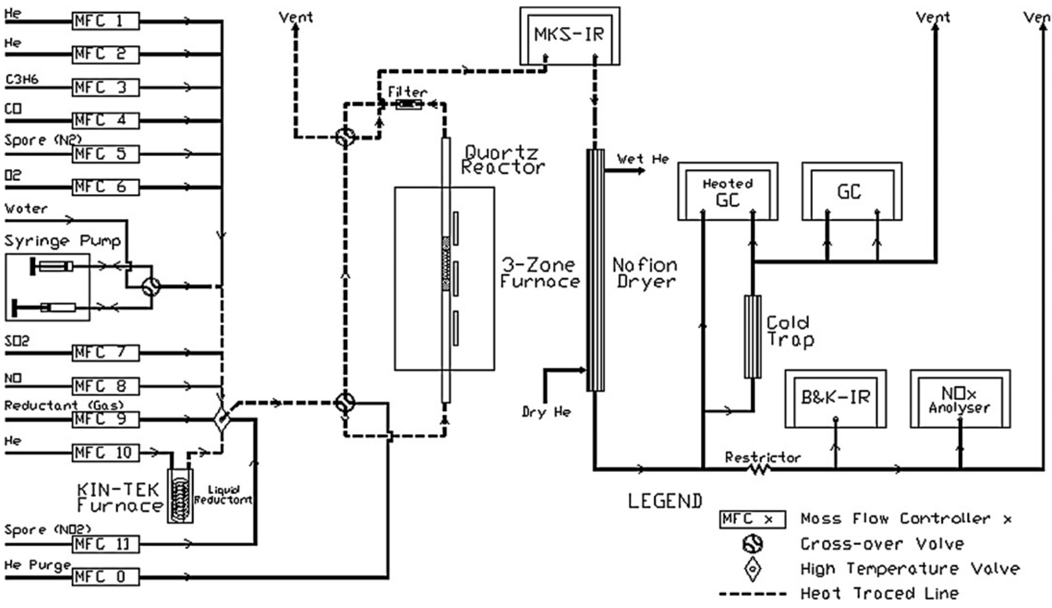

Fig. 1. DeNO$_x$ reaction system.

Table 2
Catalyst compositions by SEM/EDX.

Catalyst name	Composition (mass %)					
	Pd	Fe	Co	K	Al	Ti
Al_2O_3–TiO_2	n.a.	n.a.	n.a.	n.a.	41.5 (0.5)	12.9 (0.6)
Pd/Al_2O_3–TiO_2	0.7 (0.0)	n.a.	n.a.	n.a.	39.3 (0.2)	14.9 (0.2)
Pd/K/Al_2O_3–TiO_2	0.6 (0.1)	n.a.	n.a.	0.7 (0.0)	39.0 (0.6)	14.9 (0.6)
Pd/Co/Al_2O_3–TiO_2	0.5 (0.0)	n.a.	0.7 (0.1)	n.a.	38.4 (0.3)	15.6 (0.3)
Pd/K/Co/Al_2O_3–TiO_2	0.3 (0.0)	n.a	0.6 (0.1)	0.3 (0.0)	39.1 (0.1)	14.8 (0.1)
Pd/Fe/Al_2O_3–TiO_2	0.8 (0.2)	1.8 (0.2)	n.a	n.a	40.0 (0.6)	12.6 (0.5)

n.a.: not applicable; (. . .): standard deviation.

3.1.2. BET surface area

The surface areas of the catalysts are shown in Table 3, and decrease with increasing metal loading. The Pd/Fe formulation, which has the highest metal loading, shows a surface area considerably lower than that of the support. It is possible that excess Fe incorporation resulted in the blockage of smaller pores, resulting in a lower measured surface area.

3.1.3. X-ray diffraction

X-ray diffraction patterns for selected catalysts are shown in Fig. 2A and B. The comparison of spectra (a) and (b) in Fig. 2A reveals that they are nearly identical patterns, indicating that TiO_2 was highly dispersed over the surface of the alumina. In particular, the TiO_2 reflection near 25° (2θ) is notably absent from spectrum (b), further indicating the high dispersion of TiO_2 on the support. Spectra (c) and (d) show the XRD patterns of the Pd and Pd/Fe catalysts. Comparison of these spectra with (b) indicates that repeated calcination following the incorporation of each metal may have led to sintering of some TiO_2 of the support. This is evidenced by a weak reflection near 25° (2θ), which is characteristic of TiO_2. The presence of Pd in these two catalysts is confirmed by the presence of a reflection at 34° (2θ) in spectra (c) and (d). This feature is visible between the two alumina peaks at 32° and 37° (2θ), where the signal of PdO would be observed. This PdO peak is of increased intensity in spectrum (d), as shown in Fig. 2B. This is explained by the higher Pd content of this catalyst. There is also additional diffraction intensity in this region of the XRD spectrum of (d) as shown on the overlaid spectra in Fig. 2B. This intensity increase at 33° (2θ) suggests the presence of iron, as Fe_2O_3. Finally, a comparison of the region 35–40° (2θ) of the XRD spectra (c) and (d) reveals a slight intensity increase at about 37° (2θ), which indicates the presence of iron as FeO. This suggests that Fe maybe present in this catalyst in both (2+) and (3+) oxidation states.

Table 3
BET surface area.

Catalyst name	Surface area (m^2/g)
Al_2O_3	270.0
Al_2O_3–TiO_2	262.6
Pd/Al_2O_3–TiO_2	257.1
Pd/K/Al_2O_3–TiO_2	205.0
Pd/Co/Al_2O_3–TiO_2	218.0
Pd/K/Co/Al_2O_3–TiO_2	235.8
Pd/Fe/Al_2O_3–TiO_2	169.7

3.2. SCR activity testing

DeNO$_x$ activity data of the catalyst series are shown in Figs. 3–6. NO conversion at low temperature is readily observed over the prepared catalysts between 150 °C and 220 °C in Fig. 3. The catalyst series shows maximal NO conversion at temperatures near 200 °C, with little variation in the observed temperatures of peak activity. It could be argued that slightly better NO reduction activity is observed over the unpromoted (Pd) and Co promoted (Pd/K/Co and Pd/Co) formulations relative to the Fe (Pd/Fe) and K (Pd/K) promoted formulations. Also evident is that all of the prepared catalysts exhibit a second maximum in NO reduction activity between 250 °C and 300 °C, where significant variations in the temperatures

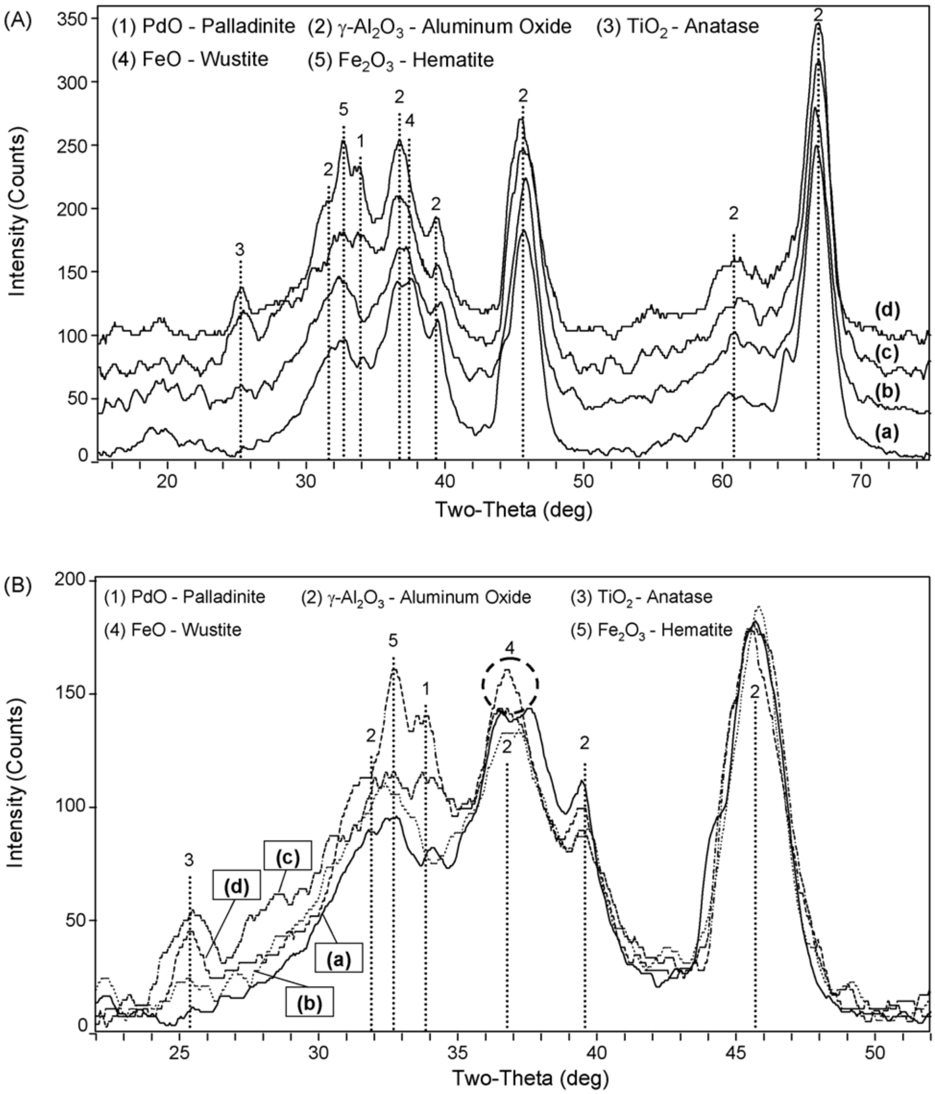

Fig. 2. (A) XRD patterns of selected catalysts supported on Al_2O_3–TiO_2: (a) γ-Al_2O_3, (b) Al_2O_3–TiO_2, (c) Pd/Al_2O_3–TiO_2 and (d) Pd/Fe/Al_2O_3–TiO_2. (B) Overlaid XRD pattern (22–52°, 2θ) of selected catalysts supported on Al_2O_3–TiO_2: (a) γ-Al_2O_3, (b) Al_2O_3–TiO_2, (c) Pd/Al_2O_3–TiO_2 and (d) Pd/Fe/Al_2O_3–TiO_2.

of peak NO reduction activity are observed. It is in this region that the effect of the promoter elements becomes clear, with the ranking of NO conversion being Pd/K/Co > Pd/Co > Pd > Pd/K > Pd/Fe. For comparison, the performance of a Pd catalyst on a similar support (90% Al_2O_3–10% TiO_2), adapted from the work of Macleod and Lambert [6] is also shown in Fig. 3. It is clear that the results of these authors show higher NO conversion at temperatures 40–50 °C lower in temperature than the catalysts in the present study. Fig. 3 reveals also that the catalysts of the present study show activity over wider ranges of temperatures and in the presence of 5 vol% water. The Pd/K/Co catalyst appears to offer the best NO conversion over the widest temperature range.

Fig. 4 shows the selectivity to N_2O of each catalyst as a function of temperature. Due to errors associated with calculating selectivity at low conversion, the activity results are presented from 125 °C to 450 °C. The effect of promoter elements is indicated by the fact

Table 4
Temperatures of the maximum conversion of NO and reductants.

Catalyst	T_{NO}[a] (°C)	Max NO conv. (%)	T_{H_2}[b] (°C)	T_{CO}[c] (°C)	N_2 selectivity at T_{NO_x} (%)
Pd/Al_2O_3–TiO_2	200	94	170	193	84
Pd/K/Al_2O_3–TiO_2	203	84	NA	192	89
Pd/Co/Al_2O_3–TiO_2	205	97	NA	182	87
Pd/K/Co/Al_2O_3–TiO_2	215	96	NA	200	88
Pd/Fe/Al_2O_3–TiO_2	189	79	170	189	87
Pd/Al_2O_3–TiO_2[d]	143	99	140	140	70

NA: not available.
[a] T_{NO} is defined as the temperature at which maximum NO conversion is observed.
[b] T_{H_2} is defined as the temperature at which complete H_2 is observed.
[c] T_{CO} is defined as the temperature at which complete CO is observed.
[d] Macleod and Lambert [6].

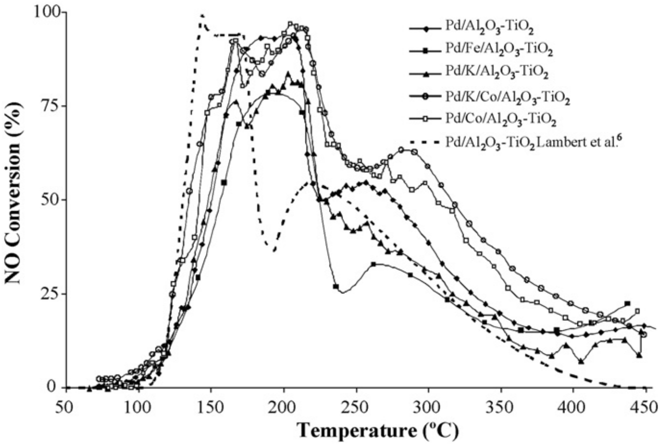

Fig. 3. NO conversion as a function of temperature.

that significantly lower N_2O selectivity is observed over the Pd/K/Co and Pd/Co formulations compared to the other formulations. Under conditions of maximum conversion of NO, near 200 °C as shown in Fig. 3, the selectivity to N_2O (Fig. 4) for all catalysts is minimal. At the second maxima of NO conversion, between 250 °C and 300 °C, as shown in Fig. 3, the Pd/K/Co catalyst shows the highest NO conversion while exhibiting the lowest N_2O selectivity in Fig. 4. This again indicates the important role played by promoter elements in this series of Pd catalysts.

Fig. 5 shows the N_2 selectivity of the catalyst series. All catalysts exhibit maximal N_2 selectivity under conditions of maximal NO conversion (near 200 °C).

These findings are summarized in Table 4, where temperatures of maximal NO reduction and reductant conversion are compared. Limited studies on H_2 conversion at steady state using gas chromatography indicate complete H_2 conversion at 170 °C, while the CO conversion temperatures varied among the different catalysts. The unpromoted Pd catalyst shows 94% NO conversion with 84% N_2 selectivity and complete CO conversion at 200 °C. The promoted Pd catalysts all exhibit higher N_2 selectivity compared to the unpromoted Pd catalyst. Also, the Pd/K/Co catalyst exhibited a higher CO light-off temperature, giving a wider temperature range of activity. In fact, as shown in Table 4, all of the catalysts exhibit T_{NO} values which exceed the T_{CO} measured in the experiment. Among the catalysts tested, the Pd/K/Co formulation shows the highest T_{CO} (200 °C), and the widest range of activity.

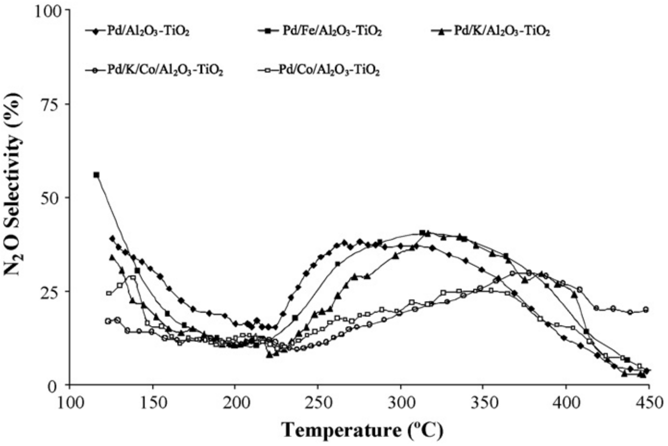

Fig. 4. Selectivity to N_2O as a function of temperature.

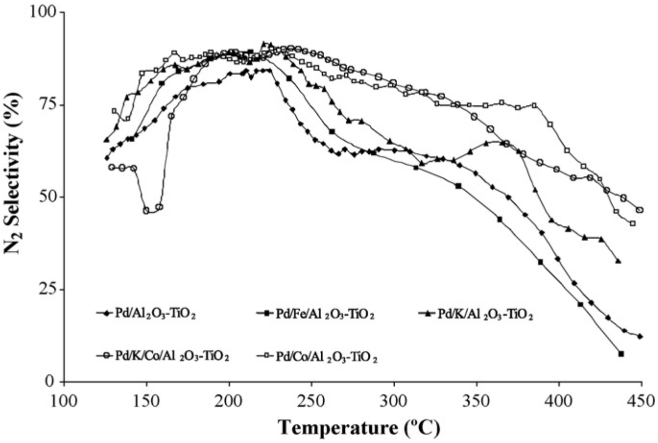

Fig. 5. Selectivity to N_2 as a function of temperature.

These results suggest that another reductant is being produced *in situ* that is responsible for NO conversion observed above T_{CO}. Previous literature reports [7–10] have suggested NH_3 precursors may form during such reactions. However, ongoing studies in our laboratory indicate that NH_3 is likely oxidized to NO_2 in the presence of noble metals at approximately 250 °C. Other authors present evidence which suggests that the intermediate maybe an alcohol. For example, Iordache-Cazana and Smith have reported the conversion of syngas to ethanol over Pd catalysts, and have identified K as a significant promoter of this reaction [17]. Furthermore, the work of Roseno et al. reports the use of ethanol as a NO_x reductant over alkali promoted Pd catalysts [18]. They report similar conversion as under the same temperature range (250–300 °C) as shown in Fig. 3.

Finally, as presented in Fig. 6, all catalysts show pronounced activity losses and increased selectivity to NO_2 at temperatures beyond 400 °C. A key question to be addressed in future work is whether the catalysts tested simply are not active at high temperature, or if these catalysts undergo a deactivation process (i.e. sintering). Durability studies in our laboratory on selected catalysts have indicated no significant activity loss across repeated testing runs, suggesting that deactivation is not the reason for the observed low activity at high temperature. We currently have no explanation for the increased selectivity to NO_2 exhibited by the Pd/K/Co catalyst between 125 °C and 175 °C.

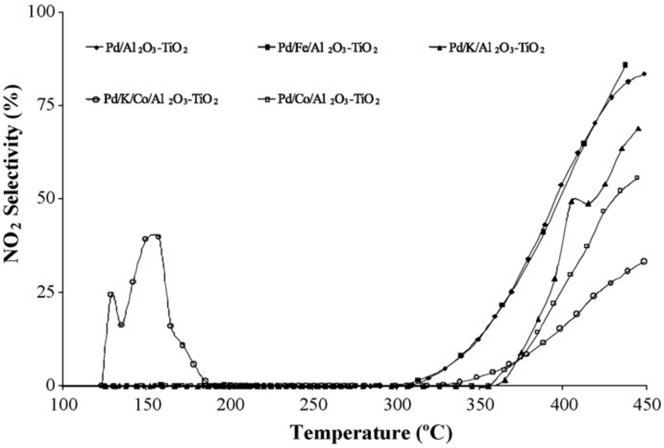

Fig. 6. Selectivity to NO_2 as a function of temperature.

4. Conclusions

The series of Fe, Co and K promoted Pd on a mixed oxide Al_2O_3–TiO_2 support shows excellent low temperature $DeNO_x$ activity using a H_2-rich syngas reductant. These catalysts show high NO reduction across a wide range of temperature. We have associated the observed low temperature ($T < 200\,^{\circ}C$) NO reduction to the H_2 component of the syngas reductant. This has been substantiated by gas chromatography measurements of H_2 conversion temperatures. The use of K and Co as promoters of Pd was found to improve N_2 selectivity at low temperature. A refinement of the relative Pd/K/Co loadings, which may lead to further increases in NO conversion and N_2 selectivity, will constitute the basis for future work.

At higher temperatures ($200\,^{\circ}C < T < 400\,^{\circ}C$), the catalysts were less active in NO reduction. We have explained this region of activity in terms of CO acting as a reductant, and again the K and Co promoted catalysts were superior. The Pd/K/Co formulation showed the highest NO reduction and the highest N_2 selectivity under these conditions.

We conclude from the $DeNO_x$ activity test results obtained by online FTIR that all catalysts maintain activity at temperatures beyond the complete conversion of CO (T_{CO}). This temperature varied among all catalysts tested, with the largest value of T_{CO} (both in absolute terms and relative to T_{NO}) exhibited by the Pd/K/Co catalyst. This result suggests that an *in situ* generated reductant is responsible for the activity beyond T_{H_2} and T_{CO}. At temperatures beyond 400 °C, the selectivity to NO_2 increases significantly. The catalysts tested are stable under these conditions as repeat testing has revealed no loss of activity (i.e. no sintering/deactivation).

In addition, other promoter elements will be studied to attempt to widen the range of $DeNO_x$ activity to higher temperatures. Finally, the SEM/EDS, BET and XRD data of the Pd/Fe catalyst indicate that excess Fe was loaded onto this catalyst during preparation. Thus, repeat studies on this particular catalyst will have to be conducted in order to conclusively evaluate the use of Fe as a promoter element for Pd-based syngas SCR catalysts.

Acknowledgements

The authors gratefully acknowledge the collaboration of Dr. Gianni Caravaggio regarding the XRD measurements, the Natural Sciences and Engineering Research Council of Canada (NSERC) for a Visiting Fellowship in Government Laboratories and the financial support from the Program of Energy Research and Development (Natural Resources Canada) through the Advanced Fuels and Transportation Emissions Reduction R&D portfolio.

References

[1] S. Roy, M. Hegde, G. Madras, Appl. Energy 86 (2009) 2283–2297.
[2] http://www.dieselnet.com/standards/us/ld_t2.php.
[3] M. Yao, Z. Zheng, H. Liu, Prog. Energy Combust. Sci. 35 (2009) 398–437.
[4] M. Zheng, G. Reader, J. Hawley, Energy Convers. Manage. 45 (2004) 883–900.
[5] N. Macleod, R.M. Lambert, Appl. Catal. B 35 (2002) 269–279.
[6] N. Macleod, R.M. Lambert, Catal. Commun. 3 (2002) 61–65.
[7] N. Macleod, R.M. Lambert, Chem. Commun. (2003) 1300–1301.
[8] N. Macleod, R.M. Lambert, Appl. Catal. B 46 (2003) 483–495.
[9] N. Macleod, R. Cropley, J.M. Keel, R.M. Lambert, J. Catal. 221 (2004) 20–31.
[10] M. Konsolakis, M. Vrontaki, G. Avgouropoulos, T. Ioannides, I.V. Yentekakis, Appl. Catal. B 68 (2006) 59–67.
[11] A. Grossale, I. Nova, E. Tronconi, D. Chatterjee, M. Weibel, J. Catal. 256 (2008) 312–322.
[12] R. Burch, M.D. Coleman, Appl. Catal. B 23 (1999) 115–121.
[13] V.N. Costa, V.C. Stathopoulos, A.M. Belessi, Efstathiou, J. Catal. 197 (2001) 350–364.
[14] A. Ueda, T. Nakao, M. Azuma, T. Kobayashi, Catal. Today 45 (1998) 135–138.
[15] T. Maunula, Y. Kintaichi, M. Inaba, M. Haneda, K. Sato, H. Hamada, Appl. Catal. B 15 (1998) 291–304.
[16] J.F. Kelly, M. Stanciulescu, J.-P. Charland, Fuel 85 (2006) 1772–1780.
[17] C. Iordache-Cazana, K. Smith, US Patent 7,384,987.
[18] K.T.C. Roseno, M.A.S. Baldanza, M. Schmal, Catal. Lett. 124 (2008) 59–67.